Supporting Information

The Role of Unfused-ring-based Small-molecule Acceptors as the Third Component in Ternary Organic Photovoltaics

Bing-Huang Jiang[1][#], Yi-Sheng Chen[2][#], Yu-Chi You[3], Yu-Wei Su[4], Chun-Yen Chang[1], Hui-Shan Shih[5], Zhong-En Shi[1], Chih-Ping Chen[1,2, 6]*, and Ken-Tsung Wong [3,7]*

[1] Department of Materials Engineering, Ming Chi University of Technology, New Taipei City 243, Taiwan

[2] Organic Electronic Research Center, Ming Chi University of Technology, New Taipei City 243, Taiwan

[3] Department of Chemistry, National Taiwan University, Taipei 10617, Taiwan

[4] Department of Molecular Science and Engineering, Institute of Organic and Polymeric Materials, National Taipei University of Technology, Taipei 106344, Taiwan

[5] Department of Chemical Engineering, Feng Chia University, Taichung40724, Taiwan

[6] College of Engineering, Chang Gung University, Taoyuan City, 33302, Taiwan, Republic of China

[7] Institute of Atomic and Molecular Science, Academia Sinica, Taipei 10617, Taiwan

[#] These authors contribute equally to this work

Experimental Section

Material

All solvents were purified by distillation using drying agents before use. Other chemicals and reagents were used as received from commercial suppliers without further purification. These included PM6 and Y6 which were purchased from Solarmer.

Synthesis of dialdehyde 1

The mixture of 4,4-bis(2-ethylhexyl)-4H-cyclopenta[2,1-b:3,4-b']dithiophene-2-carbaldehyde (0.56 g, 1.30 mmol), NTz-Br (0.26 g, 0.45 mmol), $Pd_2(dba)_3$ (0.06 g, 0.07 mmol), and potassium carbonate (0.27 g, 1.95 mmol) were treatment with a few drops of PivOH. The flask was evacuated and purged with argon gas, then the dry DMAc (13.0 mL) was added. The mixture was reacted at 70 ^{0}C overnight. After cooling temperature, the mixture was reprecipitated from $CHCl_3$/MeOH and then purification by the column chromatography on silica gel (hexane/$CHCl_3$) to afford crude product as orange-red solid. The crude product was reprecipitated again from $CHCl_3$/MeOH to give the title compound as a bright orange solid. (0.22 mg, 37%). ^{1}H NMR (400 MHz, $CDCl_3$) δ 9.84 (s, 2H), 8.71 (s, 2H), 8.19 (s, 2H), 7.60 - 7.58 (t, J = 4 Hz, 2H), 4.81 - 4.79 (d, J = 8 Hz, 4H), 2.33 (m, 2H), 2.07 - 1.95 (m, 8H), 1.41 - 1.33 (m, 14H), 1.03 - 0.90 (m, 46H), 0.75 - 0.71 (t, J = 8 Hz, 10H), 0.65 - 0.61 (m, 18H) ; ^{13}C NMR (100

MHz, CDCl$_3$) δ 182.48, 162.87, 158.03, 157.98, 148.03, 144.46, 143.38, 142.51, 140.61, 136.91, 130.64, 124.28, 122.77, 122.22, 117.48, 59.84, 54.23, 43.20, 40.59, 35.37, 34.38, 34.14, 30.63, 28.57, 28.49, 27.58, 27.34, 24.03, 22.96, 22.76, 22.71, 14.09, 14.03, 13.93, 10.72, 10.60 ; HRMS (m/z, MALDI, [M]$^+$) Calcd for C$_{78}$H$_{110}$N$_6$O$_2$S$_4$ 1290.7573, found 1291.7698.

Synthesis of NTzCPDTCN

To a two-neck round-bottom flask was added 10 (x g, y mmol), malononitrile (0.35 g, 5.40 mmol) and flask was evacuated and purged with argon gas, then chloroform (13 mL) was added. The pyridine (0.9 mL) was slowly added dropwise, and gently heated at 65 °C for 48 hr. After cooling temperature, the mixture was reprecipitated from CHCl$_3$/MeOH and then purification by the column chromatography on silica gel (CHCl$_3$) to afford crude product as brown solid. The crude product was reprecipitated again from CHCl$_3$/MeOH to give the title compound as a deep brown solid. (0.04 g, 74%). ^{1}H NMR (400 MHz, CDCl$_3$) δ 8.75 (s, 2H), 8.23 (s, 2H), 7.75 - 7.73 (t, J = 4 Hz, 2H), 7.62 - 7.57 (t, J = 10 Hz, 2H), 4.84 - 4.82 (d, J = 8 Hz, 4H), 2.36 (m, 2H), 2.11 - 1.99 (m, 8H), 1.44 - 1.35 (m, 14H), 1.05 - 0.91 (m, 46H), 0.81 - 0.73 (m, 10H), 0.68 - 0.63 (m, 18H) ; ^{13}C NMR (100 MHz, CDCl$_3$) δ 164.64, 150.01, 146.81, 142.48, 140.52, 136.62, 135.64, 131.51, 124.18, 122.82, 122.48, 117.94, 115.14, 114.55, 72.21, 59.93, 54.35, 43.17, 40.59, 35.48, 34.31, 34.13, 30.61, 28.53, 28.47, 27.51, 27.32, 24.01, 22.95, 22.78, 22.70, 14.08, 14.03, 13.92, 10.68, 10.60 ; HRMS (m/z, MALDI, [M]$^+$) Calcd for C$_{84}$H$_{110}$N$_{10}$S$_4$ 1386.7798, found 1387.7833.

Device Fabrication

The OPVs employed a inverted sandwich structure with the following layers: glass/ITO/ZnO/active layer/MoO$_3$/Ag. The patterned ITO-coated glass substrates (resistance: 6.4 Ω sq^{-1}) were sequentially cleaned with deionized (DI) water, acetone, and isopropanol using an ultrasonic bath (DELTA, DC200H) for 20 minutes. A sol-gel ZnO precursor solution was prepared by stirring a mixture of zinc acetate (3.15 g), ethanolamine (0.9 mL), and 2-methoxyethanol (29.1 mL) at 25 °C for 3 days. Prior to ZnO deposition, the glass/ITO substrate was treated with oxygen plasma (Harrick Plasma, PDC-32G) for 5 minutes. The ZnO precursor solution was then filtered through a 0.45 μm filter and spin-coated onto the glass/ITO substrate in air. Subsequently, the sample was annealed at 160 °C for 10 minutes to form a ZnO layer with a thickness of approximately 30 nm. The binary precursor solution for active layer was prepared via dissolving PM6 as the donor and Y6 as the acceptor (weight ratio, 1:1.2) in a solvent of CF (7.3mg/ml for donor) with 0.5% 1-chloronaphthalene (CN); stirring at 60 °C overnight in an Ar-filled glove box. The ternary precursor solution for active layer was

prepared via dissolving PM6, Y6, and **NTzCPDTID** (**NTzCPDT2F**, or **NTzCPDTCN** as guest acceptor (weight ratio, 1:1.2:0.1) in a solvent of CF (7.3mg/ml for donor) with 0.5% 1-chloronaphthalene (CN); stirring at 60 °C overnight in an Ar-filled glove box. The active layer was then deposited onto the glass/ITO/ZnO substrate at room temperature. The thickness of the active layer was optimized by controlling the spin speed and the concentration of the precursor solution. Using evaporation equipment under a vacuum of $<10^{-6}$ torr, a 3 nm MoO_3 layer and a 100 nm Ag layer were deposited onto the active layer to complete the device. The active area of 0.1 cm^2 was defined by the overlap between the ITO and Ag electrodes.

Characterization

UV-vis absorption spectra and photoluminescence (PL) spectra were obtained using a Jasco V-650 UV-vis spectrophotometer and an Edinburgh FLS1000 photoluminescence spectrometer, respectively. Current density-voltage (J-V) curves of the OPV devices were measured inside a glovebox using a Keithley 2400 source measurement system and an Enlitech AAA Class solar simulator (allowing light intensity control from 10 to 100 mW/cm²). External quantum efficiency (EQE) spectra were measured with a QE-R Solar Cell Spectral Response Measurement System (Enli Technology Co., Ltd., Taiwan). The system employs two certified photodetectors (Si and Ge) for monochromatic light calibration. Surface morphologies of the blend films were investigated by atomic force microscopy (AFM) in tapping mode at room temperature using a Bruker Dimension Edge microscope. GIWAXS was performed at the TLS-BL23A beamline of the National Synchrotron Radiation Research Center (NSRRC) in Taiwan (X-ray wavelength: 0.83 Å; incident angle: 0.12°). The FTPS-EQE spectra of binary and ternary OPVs were recorded using an integrated system, PECT-600 (Enli Technology Co., Ltd., Taiwan). Similarly, the EL and EQEEL spectra were recorded using another integrated system, ELCT-3010 (Enli Technology Co., Ltd., Taiwan), by applying an external voltage of 0–5 V to the corresponding OPV cells. Photovoltaic properties, including photo-CELIV, transient photocurrent (TPC), and transient photovoltage (TPV) measurements, were determined using an all-in-one Paios characterization platform (Fluxim AG).
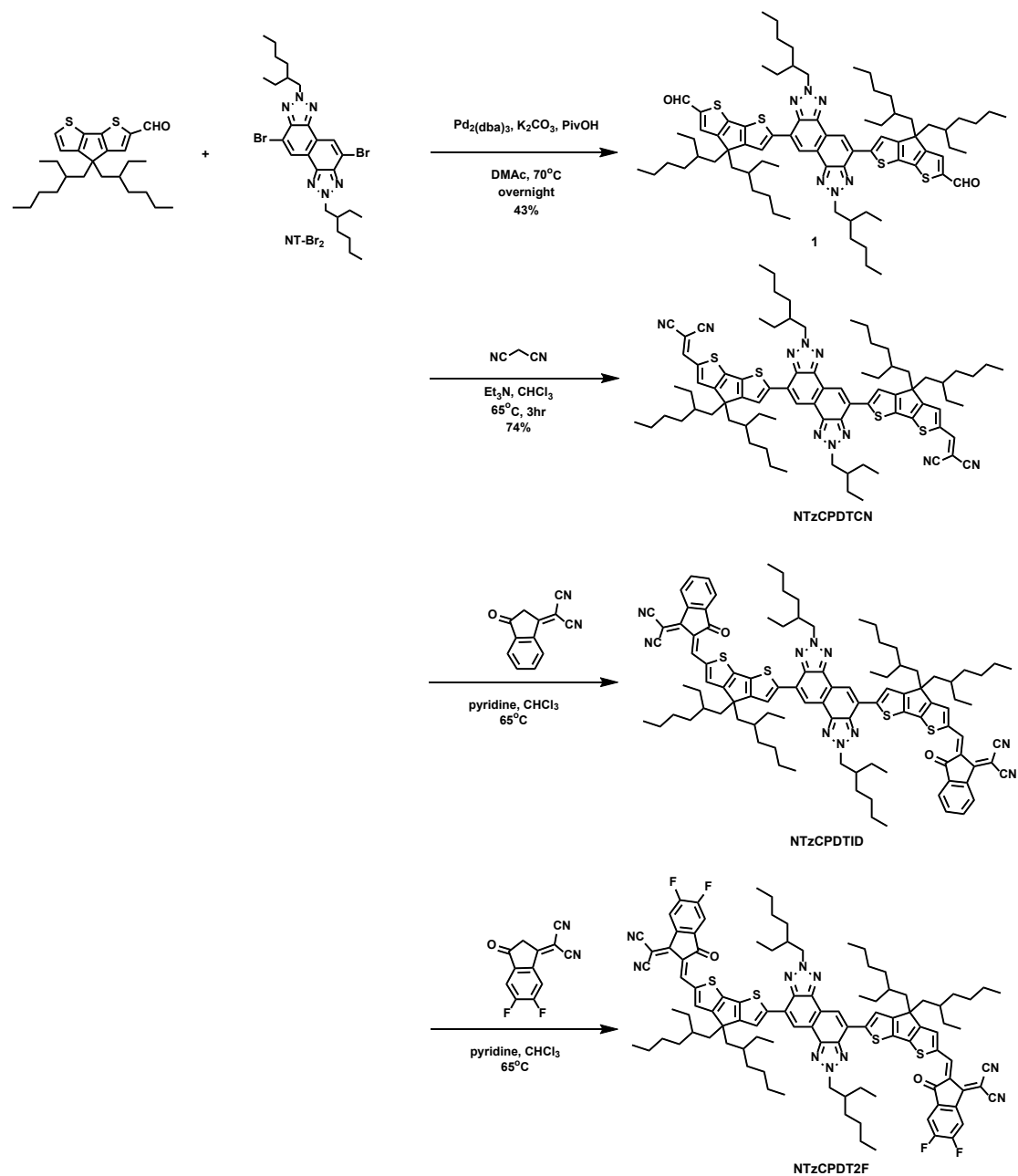
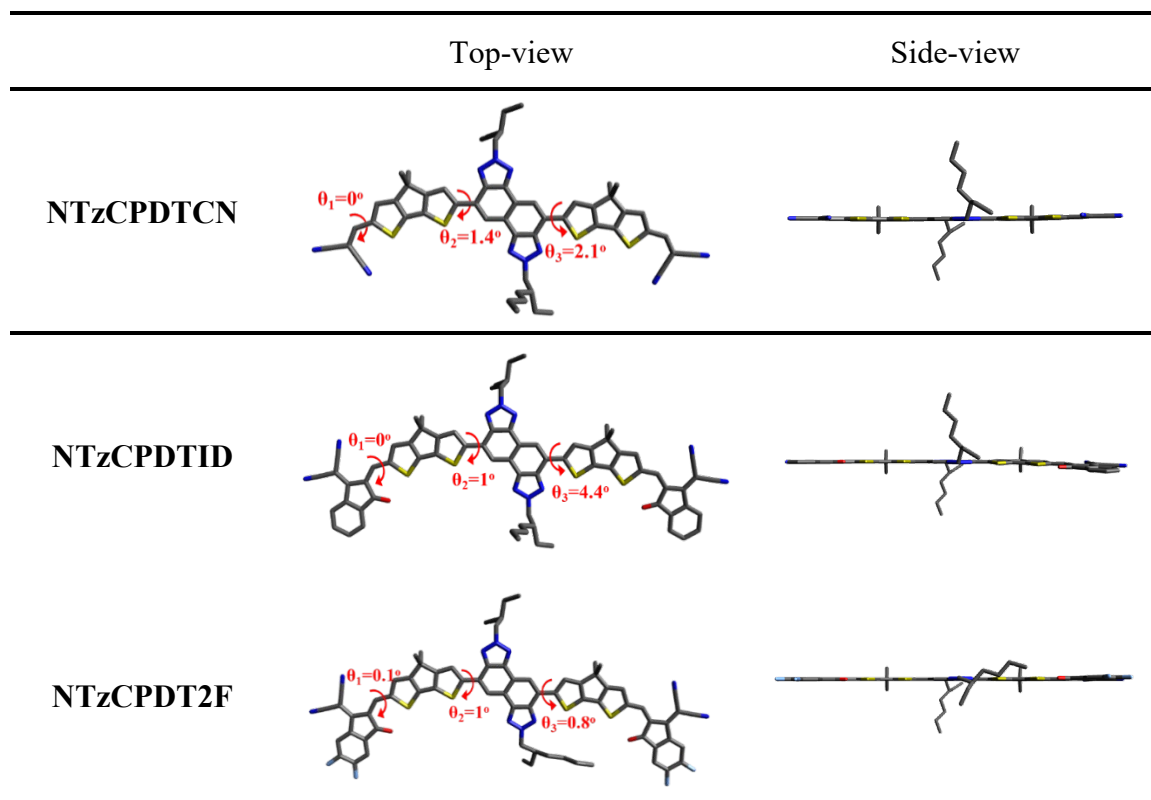**Scheme S1.** Synthesis of **NTzCPDTCN**, **NTzCPDTID**, **NTzCPDT2F** acceptors.

Figure S1. (a)1H NMR and (b)13C NMR spectra of **NTzCPDTCN**.

	Top-view	Side-view
NTzCPDTCN	$\theta_1=0°$ $\theta_2=1.4°$ $\theta_3=2.1°$	
NTzCPDTID	$\theta_1=0°$ $\theta_2=1°$ $\theta_3=4.4°$	
NTzCPDT2F	$\theta_1=0.1°$ $\theta_2=1°$ $\theta_3=0.8°$	

Figure S2. The optimized structure of NTz-based acceptors (a) top-view (b) side-view

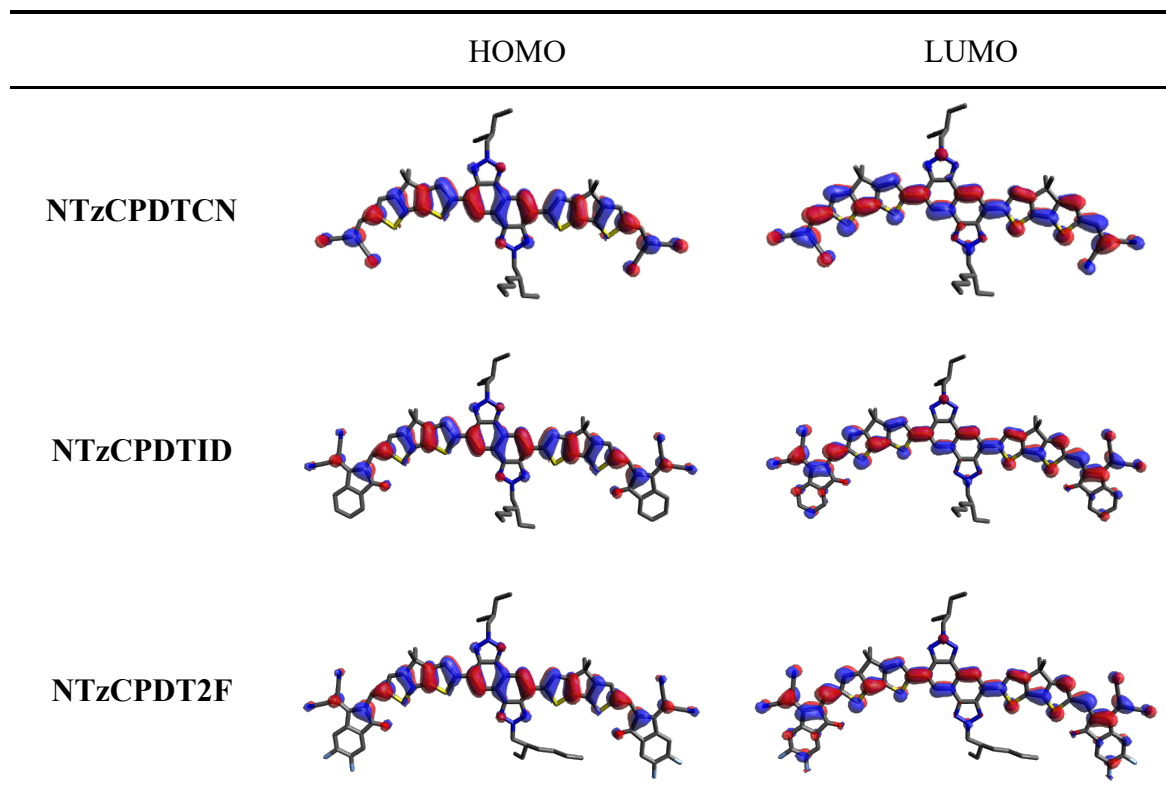|	HOMO	LUMO
NTzCPDTCN		
NTzCPDTID		
NTzCPDT2F		

Figure S3. The HOMO and LUMO distributions of NTz-based acceptors
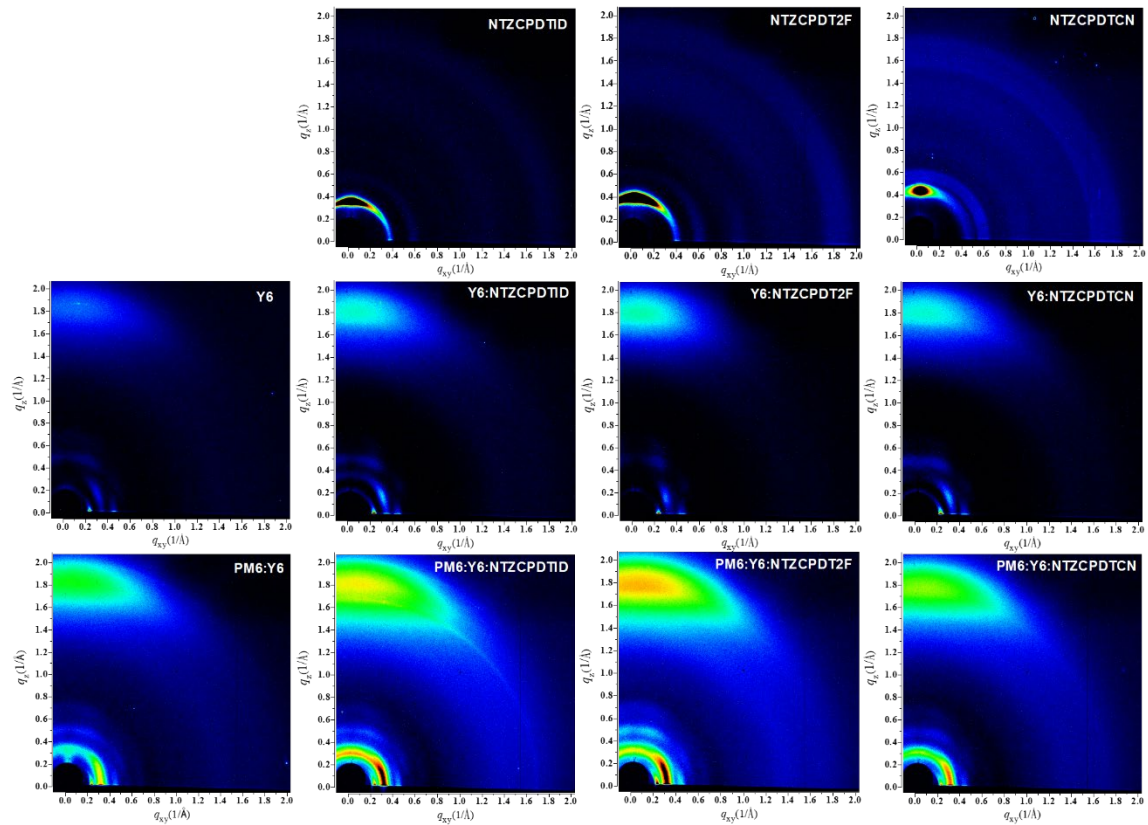
Figure S4. 2D GIWAXS patterns of the neat, acceptor blend, PM6:Y6 blend, and ternary blend films.
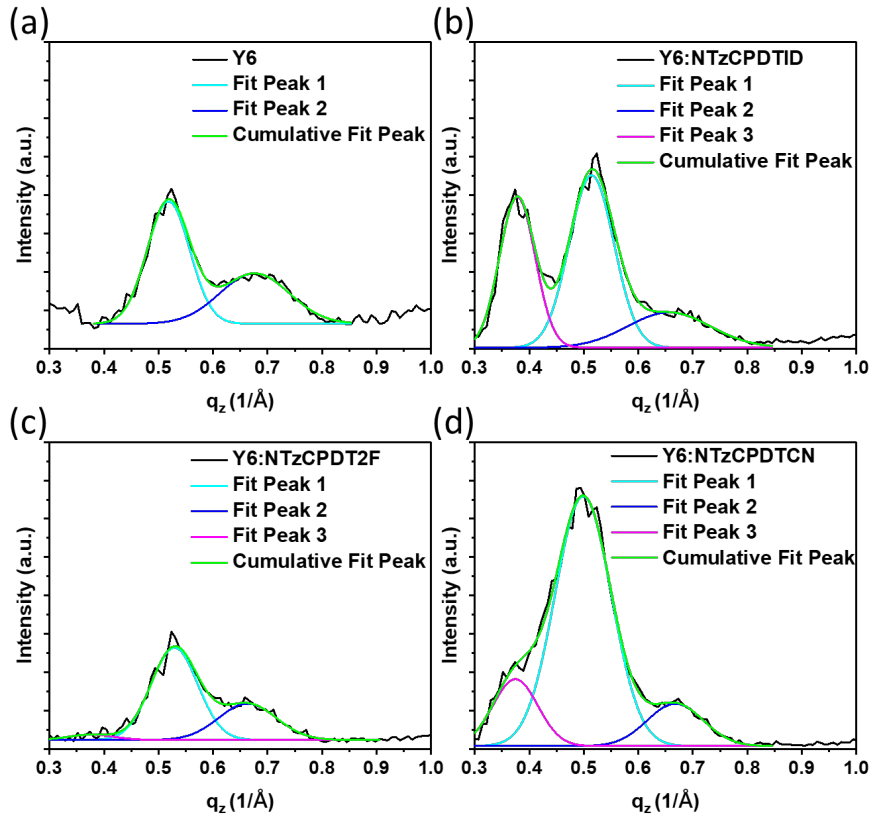
Figure S5. The zoom-in 1D GIWAXS profile (black line) of (a) Y6, (b)Y6:**NTzCPDTID** (c) Y6:**NTzCPDT2F** (d) Y6:**NTzCPDTCN** films. The profile can be fitted by using two or three Gaussian functions.

Table S1. Detailed Energy loss parameters of the binary and ternary OPVs.

Active layer	E_{gap} [eV]	qV_{OC} [eV]	E_{loss} [eV]	E_{CT} [eV]	ΔE_{CT} [eV]	ΔE_{rad} [eV]	$\Delta E_{non-rad}$ [eV]	EQE_{EL}
PM6:Y6	1.432	0.868	0.564	1.386	0.046	0.266	0.252	5.5×10^{-5}
PM6:Y6:**NTzCPDTID**	1.428	0.874	0.554	1.417	0.011	0.266	0.277	2.1×10^{-5}
PM6:Y6:**NTzCPDT2F**	1.433	0.885	0.548	1.394	0.039	0.266	0.243	7.8×10^{-5}
PM6:Y6:**NTzCPDTCN**	1.430	0.879	0.551	1.408	0.022	0.266	0.263	3.6×10^{-5}